Physica B 405 (2010) 2357–2361

Contents lists available at ScienceDirect

Physica B

journal homepage: www.elsevier.com/locate/physb

The structural, electronic and optical properties of $In_xGa_{1-x}P$ alloys

M. Othman [a,*], E. Kasap [a], N. Korozlu [b]

[a] Gazi University, Department of Physics, Teknikokullar, 06500 Ankara, Turkey
[b] Erzincan University, Department of Physics, Basbaglar, 24100 Erzincan, Turkey

ARTICLE INFO

Article history:
Received 22 September 2009
Received in revised form
15 February 2010
Accepted 20 February 2010

Keywords:
Alloys
Electronic structure
Optical properties

ABSTRACT

The structural, electronic energy band structure and linear optical properties $In_xGa_{1-x}P$ alloys are investigated by an *ab initio* pseudopotential method using density functional theory in the local density approximation (LDA) and a scissors approximation. For these alloys lattice parameters, bulk modulus, band gap energy and density of state (DOS) are calculated. Electronic band structure shows that $In_xGa_{1-x}P$ alloys are direct band gap and the optical band gap decrease from 2.10 to 1.41 eV with increase in In concentrations. The linear energy dependent dielectric functions and some optical properties such as energy loss function, absorption and refractive index are calculated. Our results agree well with the available data in the literature.

© 2010 Elsevier B.V. All rights reserved.

Contents

1. Introduction . . . 2357
2. Method of calculation . . . 2358
3. Results and discussion . . . 2358
   3.1. Structural and electronic properties . . . 2358
   3.2. Optical properties . . . 2359
4. Conclusions . . . 2361
Acknowledgements . . . 2361
References . . . 2361

1. Introduction

At present, III–V compound semiconductors provide the materials basis for a number of well-established commercial technologies, as well as new cutting-edge classes of electronic and optoelectronic devices. Just a few examples include high-electron-mobility and heterostructure bipolar transistors, diode lasers, light-emitting diodes, photodetectors, electro-optic modulators, and frequency-mixing components [1–4]. The operating characteristics of these devices depend critically on the physical properties of the constituent materials, which are often combined in quantum heterostructures containing carriers, are confined to dimensions on the order of a nanometer. A seemingly limitless flexibility is now available to the quantum heterostructure device designer $In_xGa_{1-x}P$ alloys have been the subject of various experimental and theoretical studies recently and in the past decades. Cheng et al. [5] analyzed that surfaces are prepared by metal organic vapor phase epitaxy. Hayashi et al. [6] studied some structural and optical properties of $In_xGa_{1-x}P$ alloys. Urgaftman and Meyer [7] studied band parameters for III–V compound semiconductors and their alloys. Fredj et al. [8] studied band gap in semiconductor materials. Mori and Fitzgerald [9] studied interface disorder of $In_xGa_{1-x}P$/GaAs multiple quantum wells grown by using molecular-beam epitaxy.

Today, the production and the use with technological devices of GaP-based, In added semiconductor, which become more important gradually, increase more and more. Experimental studies on such type of produced semiconductor alloys are carried out intensively. This study was carried out to shed light on the future studies of scientists who experimentally prepare and test these alloys in laboratories, to help them in determining the change in amounts of additives in alloys, and to determine the accordance of theoretical studies with experiments and other theoretical works. To this end, features of new semiconductor

* Corresponding author. Tel.: +90 31 2 202 36 83; fax: +90 3 1 2 212 22 79.
E-mail address: mazin@gazi.edu.tr (M. Othman).

0921-4526/$ - see front matter © 2010 Elsevier B.V. All rights reserved.
doi:10.1016/j.physb.2010.02.051

alloys that may be obtained by adding In to GaP structure at various ratios were examined.

In this work, we have aimed to provide some additional information to the existing data on the physical properties of $In_xGa_{1-x}P$ alloys by using the first-principles plane-wave pseudopotential method, and we have especially focused on the electronic and optical properties. The obtained results are compared with the previous theoretical calculations and available experimental findings. The layout of this paper is given as follows: The method of calculation is given in Section 2. The results and overall conclusion are presented and discussed in Sections 3 and 4, respectively.

2. Method of calculation

The physical properties of $In_xGa_{1-x}P$ ternary alloys are investigated using the CASTEP program [10]. The model wurtzite $In_xGa_{1-x}P$ ternary alloys are used. We apply a 16-atom super-cell which corresponds to a $2\times2\times1$ that is twice the size of the primitive wurtzite unit cell in basic plane direction. In this program the calculation is performed using Kohn–Sham formation [11], which is based on the density function theory (DFT). Local density approximation (LDA) is made for electronic exchange-correlation potential energy. Coulomb potential energy, which is caused by electron–ion interaction, is described using pseudo-potential concept. The optimized non-local pseudo–potential is generated using the scheme proposed by Liuo et al. [12]. All the electronic structure calculations were performed in a super cell geometry using norm-conserving pseudo–potentials as described by Agrawal et al. [13]. The orbitals of Ga ($3d^{10}\ 4s^2\ 4p^1$), In ($4d^{10}\ 5s^2\ 5p^1$) and P ($3s^2\ 3p^3$) are treated as valence electrons.

A cubic unit cell is constructed with four group III atoms (Ga/In) and four group V atoms (P). We have considered $In_xGa_{1-x}P$ ternary alloys as having cubic symmetry in our calculation for all the five systems to maintain consistency and simplicity. We expect that for x=0.5 the alloy is a layered structure and should be non-cubic. We have taken four layers and hence a cubic unit cell for x=0.25, 0.50 and 0.75, we have replaced one, two and three Ga atoms, respectively, by In to get the desired concentration. The idea of constructing an alloys by taking a large unit cell (cubic eight–atom) and repeating it three dimensionally for the calculation of the electronic structure of the semiconductor alloy has been used by Agrawal [13] have used an eight–atom cubic super cell to calculate the electronic properties of $In_xGa_{1-x}P$ alloys. The wave functions are expanded in the plane waves up to a kinetic energy cutoff of 880 eV. In this work, the k-points of $6\times6\times4$ for x=0.5 and $4\times4\times4$ for the other composition x and y. For each $In_xGa_{1-x}P$ in this study, once the ratio between the In, Ga atoms is specified, the CASTEP simulation program randomly determines the geometrical arrangement of In–Ga atoms. In this simulation program, the chosen structural properties are the equilibrium lattice constant (a_0), bulk modulus (B_0), the energy gap at the Γ point (E_g) and optical constant for crystalline GaP, InP and $In_xGa_{1-x}P$ in the bulk structure using electronic exchange correlation energy.

Geometry optimization is performed for $In_xGa_{1-x}P$ with symmetry P1. Atomic positions are relaxed and optimized with a density mixing scheme [14] using the conjugate-gradient (CG) method [15] for eigenvalues minimization. The iteration is repeated until the energy becomes less than 0.002 meV/atom and the RMS stress becomes less than 0.1 GPa. The Monkhorst–Pack scheme [16] with uniform mesh points is applied. The wave functions are expanded in the plane waves up to a kinetic energy cutoff of 880 eV. In this paper, the k-points of $6\times6\times4$ for x=0.5 and $4\times4\times4$ for the other composition x, which are in the Monkhorst and Pack scheme, are used.

3. Results and discussion

3.1. Structural and electronic properties

As the first step in the calculations, the lattice constants of alloys at equilibrium are calculated by minimizing the lattice parameter of the crystal. Besides, bulk module is also calculated for each structure. Table 1 shows the calculated lattice constants and bulk modulus for each x of $In_xGa_{1-x}P$ along with the other experimental and theoretical values [6,17,18]. The lattice parameters are found to be 5.50, 5.53, 3.91, 5.63 and 5.72 Å for $In_xGa_{1-x}P$ alloys for x=0, 0.25, 0.5, 0.75 and 1, respectively. The lattice constant linearly increases as if the composition x increases. This is increasing many stems from the higher mass of In atom than the Ga atom. The calculated lattice constants are higher (about 2%) for GaP compound than the other theoretical and experimental findings in Refs. [8,17]. Our lattice constant for InP is about 1% higher than the other theoretical finding in Ref. [18] for composition x (x=0.25, 0.5, 0.75). These small differences of many stems from the different density functional are based on electronic structure methods. The InP has the largest lattice constant (5.72 Å), and $In_{0.5}Ga_{0.5}P$ has the smallest (3.91 Å) one for $In_xGa_{1-x}P$ x.

In the present case, the calculated bulk modulus for x=0, 0.25, 0.5, 0.75 and 1 are 90.42, 87.12, 85.48, 80.11 and 78.77, respectively. We can see that the order of compressibility from low to high is $GaP < In_{0.25}Ga_{0.75}P$, $In_{0.25}Ga_{0.75}P < In_{0.5}Ga_{0.5}P$, $In_{0.5}Ga_{0.5}P < In_{0.75}Ga_{0.25}P$ and $In_{0.75}Ga_{0.25}P < GaP$. For these configurations, the largest value of bulk modulus (90.42 GPa) is obtained for InP, therefore it has the lowest compressibility and it may be a less compressible alloy.

We have predicted the band structure for $In_xGa_{1-x}P$ along the high symmetry directions in the first Brillouin zone and corresponding density of states from the calculated equilibrium lattice constant. For all compositions (x), the calculated band structures and DOS are compatible with each other. The bands and DOS graphs are given in Fig. 1 only for x=0.25 to save space in journal. All these mixed crystals have a direct band gap along the Γ direction, and the obtained results are listed in Table 2 along with the other theoretical data [5–7,17,18]. The band profiles and band gap values are in good agreement with the earlier theoretical works. The band gaps are smaller than the experimental values because of the use of the LDA in our calculations. The energies of band gaps versus composition x (0, 0.25, 0.5, 0.75 and 1) for $In_xGa_{1-x}P$ are shown in Fig. 2. Here the composition dependence of band gap energy exhibits almost a linear decreasing trend.

Table 1
Calculated equilibrium lattice constants (a_0, c_0), bulk modulus (B), and other experimental and theoretical works for $In_xGa_{1-x}P$.

Materials	Structure	Reference	a_0 (Å)	c_0 (Å)	B (GPa)
GaP	Zinc-blende	Present	5.50	…	90.42
		Theory[a]	5.32	…	92.10
		Theory[b]	5.35	…	97.80
		Theory[c]	5.45	…	…
		Expt.[a]	5.45	…	88.00
$In_{0.25}Ga_{0.75}P$	Sulvanite	Present	5.53	…	87.12
$In_{0.5}Ga_{0.5}P$	Tetragonal *p4m2*	Present	3.90	5.58	85.48
$In_{0.75}Ga_{0.25}P$	Sulvanite	Present	5.63	…	80.11
InP	Zinc-blende	Present	5.72	…	78.77
		Theory[a]	5.72	…	73.66
		Theory[b]	5.70	…	76.10
		Theory[c]	5.85	…	…
		Expt.[a]	5.86	…	72.00

[a] Ref. [8].
[b] Ref. [18].
[c] Ref. [17].

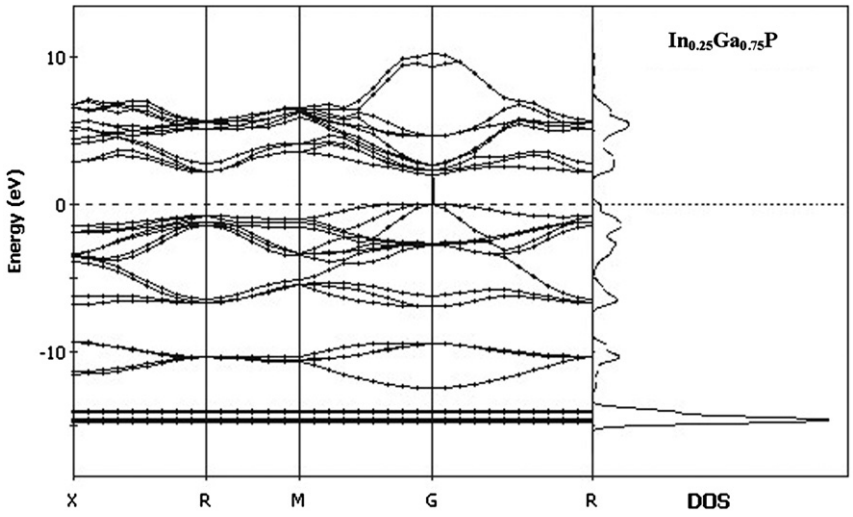

Fig. 1. Calculated band structure and DOS of $In_{0.25}Ga_{0.75}P$. The position of the Fermi level is at 0 eV.

Table 2
Band gap energies of $In_xGa_{1-x}P$.

Materials	Structure	Reference	E_g (eV)
GaP	Zinc-blende	Present	2.10
		Theory[a]	2.43
		Theory[c]	2.78
		Expt.[b]	2.23
$In_{0.25}Ga_{0.75}P$	Sulvanite	Present	1.90
$In_{0.50}Ga_{0.50}P$	Tetragonal	Present	1.71
	p4m2	Expt.[e]	1.93
$In_{0.75}Ga_{0.25}P$	Sulvanite	Present	1.52
InP	Zinc-blende	Present	1.22
		Theory[d]	1.23
		Theory[c]	1.34
		Expt.[b]	1.41

[a] Ref. [7].
[b] Ref. [17].
[c] Ref. [6].
[d] Ref. [5].
[e] Ref. [18].

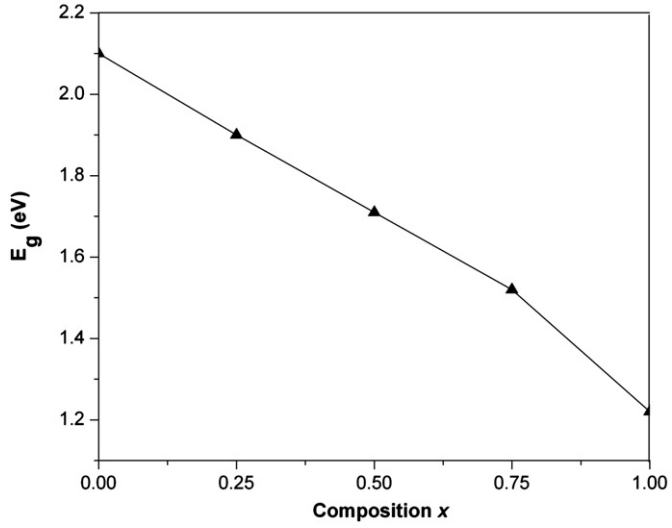

Fig. 2. Band gap energies of $In_xGa_{1-x}P$.

3.2. Optical properties

We now consider the optical properties for $In_xGa_{1-x}P$. The dielectric function $\varepsilon(\omega)=\varepsilon_1(\omega)+i\varepsilon_2(\omega)$ can be used to describe the linear response of the system to electromagnetic radiation, which relates to the interaction of photons with electrons [19]. The real $\varepsilon_1(\omega)$ and imaginary part $\varepsilon_2(\omega)$ of the dielectric functions are calculated using the usual Kramers–Kronig relationship [20]. Other optical properties can be derived from the complex dielectric function. Expressions are used for the dielectric functions, refractive index $n(\omega)$, the extinction coefficient $k(\omega)$, and energy loss function $L(\omega)$, they are given as the following [21,22]:

$$\varepsilon_1(\omega)=1+\frac{2}{\pi}\int_0^{\infty}\frac{\varepsilon_2(\omega')\omega' d\omega'}{\omega'^2-\omega^2} \tag{1}$$

$$\varepsilon_2(\omega)=\frac{Ve^2}{2\pi\hbar m^2\omega^2}\int d^3k\sum_{nn'}|\langle kn|p|kn'\rangle|^2 f(kn)\times[1-f(kn')]\partial(E_{kn}-E_{kn'}-\hbar\omega) \tag{2}$$

where $\hbar\omega$ is the energy of the incident photon, p is the momentum operator, $(\hbar/i)(\partial/\partial x)$, $|kn\rangle$ is the eigenfunction with eigenvalue E_{kn} and $f(kn)$ is the Fermi distribution function:

$$n(\omega)=\frac{1}{\sqrt{2}\left[\sqrt{\varepsilon_1^2(\omega)+\varepsilon_2^2(\omega)}+\varepsilon_1\right]^{1/2}} \tag{3}$$

$$k(\omega)=\frac{1}{\sqrt{2}\left[\sqrt{\varepsilon_1^2(\omega)+\varepsilon_2^2(\omega)}+\varepsilon_1\right]^{1/2}} \tag{4}$$

$$L(\omega)=-\mathrm{Im}(1/\varepsilon)=\varepsilon_2(\omega)/\left[\varepsilon_1^2(\omega)+\varepsilon_2^2(\omega)\right] \tag{5}$$

$$\alpha(\omega)=\sqrt{2\omega}\left[\sqrt{\varepsilon_1^2(\omega)+\varepsilon_2^2(\omega)}-\varepsilon_1(\omega)\right]^{1/2} \tag{6}$$

$$R(\omega)=\left[\frac{\sqrt{\varepsilon_1^2(\omega)+j\varepsilon_2^2(\omega)}-1}{\sqrt{\varepsilon_1^2(\omega)+j\varepsilon_2^2(\omega)}+1}\right]^2, \tag{7}$$

By using this relations [Eqs. (1)–(5)], dielectric functions $\varepsilon_1(\omega)$, $\varepsilon_2(\omega)$, refractive index $n(\omega)$ and the energy loss function $L(\omega)$ are

calculated. The present results for $In_xGa_{1-x}P$ are displayed in Fig. 3(a,b) in the range of 0–20 eV, where they represent the real part $\varepsilon_1(\omega)$ and imaginary part $\varepsilon_2(\omega)$, respectively. Fig. 3 (a) in the range of 0–20 eV, the main peaks of the real part for $In_xGa_{1-x}P$ occur at 3.50, 3.60, 3.70, 3.86 and 4.10 eV, respectively. The same peaks reduce due to the interband transition and approaches to the minimum at about 5 eV for each composition x. For each composition x (x=0, 0.25, 0.50, 0.75 and 1.0) the static dielectric constant $\varepsilon_1(0)$ are found to be 9.8, 9.7, 8.3, 9.6 and 8.4. For the imaginary part of the dielectric function is very important for optical properties of any materials. The prominent peaks occur at about 5.1, 5.2, 5.3, 4.8 and 4.6 eV for $In_xGa_{1-x}P$, respectively. These points are $\Gamma_v-\Gamma_c$ splitting, which gives the threshold for direct optical transitions between the absolute valence band maximum and the first conduction band minimum.

Fig. 4 gives the optical absorption spectra of the $InGa_{1-x}P_x$ system under the scissor operation in the range of 0–7 eV. Due to the underestimation of the band gap, it is difficult to obtain the exact optical band gap. In our calculations, we have used the energy scissor approximation with 0.6 eV to fit the absorption edge to the experimental value. This method is effective for a variety of systems [23]. The absorption starts at about 2.3, 2.0, 1.8, 1.78 and 1.61 eV for each composition x, respectively. It is well known that the relation between the optical band gap and the absorption coefficient is given by [24]:

$$\alpha h\nu = c(h\nu - E_g)^{1/2} \tag{8}$$

where h is the Planck constant, c is a constant for a direct transition, ν is the frequency of radiation and α is the optical absorption coefficient. The optical band gap E_g can be obtained from the intercept of $(\alpha h\nu)^2$ versus photon energy ($h\nu$). By using the extrapolation, the optical band gap of $InGa_{1-x}P_x$ can be obtained.

The optical band gap depending on the In concentration has been shown in the inset. It can be observed that the optical band gap decreases from 2.1 to 1.42 eV with increase in In concentrations, which is in good agreement with the previous experimental investigations [25].

Figs. 5 and 6 gives the optical constants of $InGa_{1-x}P_x$ alloys in the range of 0–20 eV. The optical constants, such as loss function and refractive index, are very important for the optical materials and related applications. Overall, the optical constants of the $InGa_{1-x}P_x$ alloys have slightly changed. For example, the energy

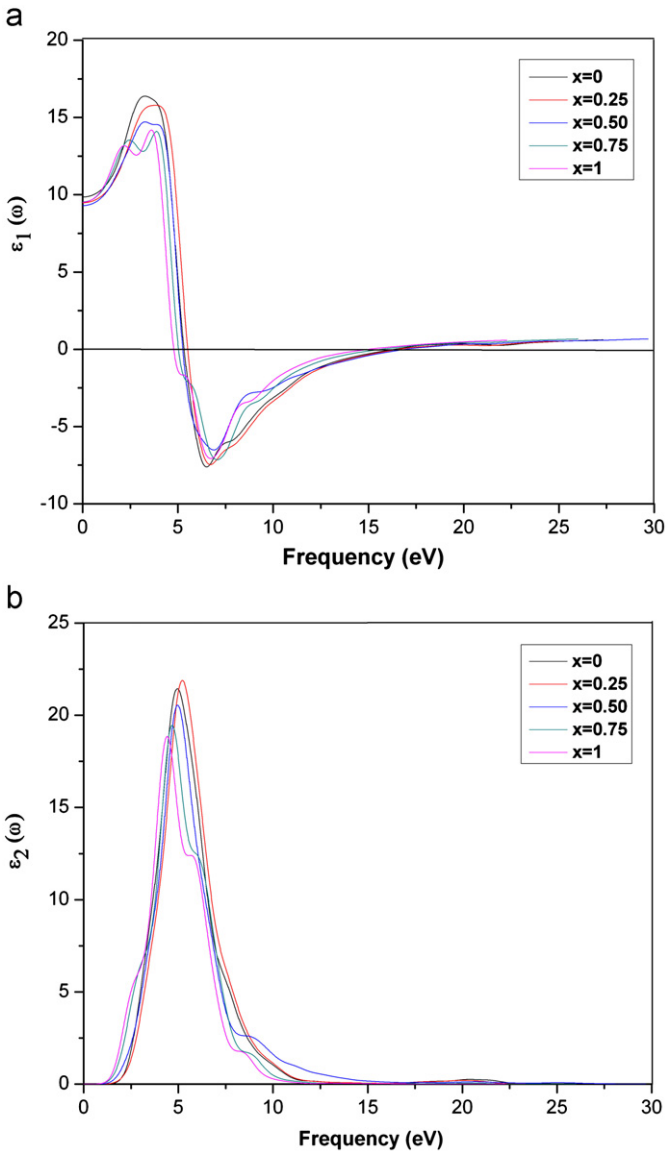

Fig. 3. (a) The real and (b) imaginary parts of dielectric function.

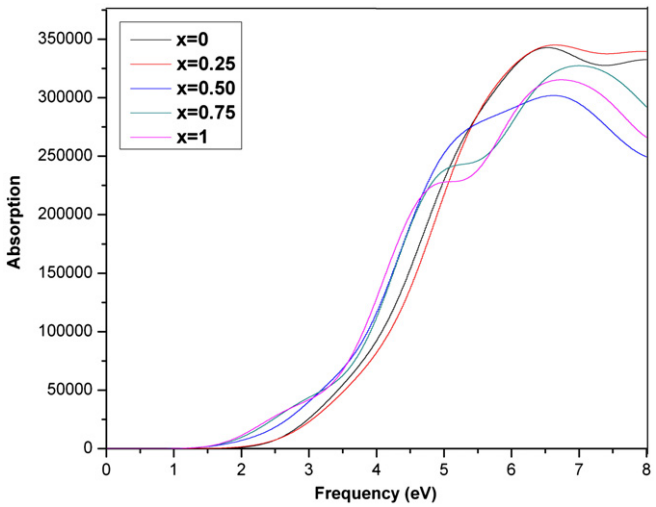

Fig. 4. Optical absorption of $In_xGa_{1-x}P$ alloys.

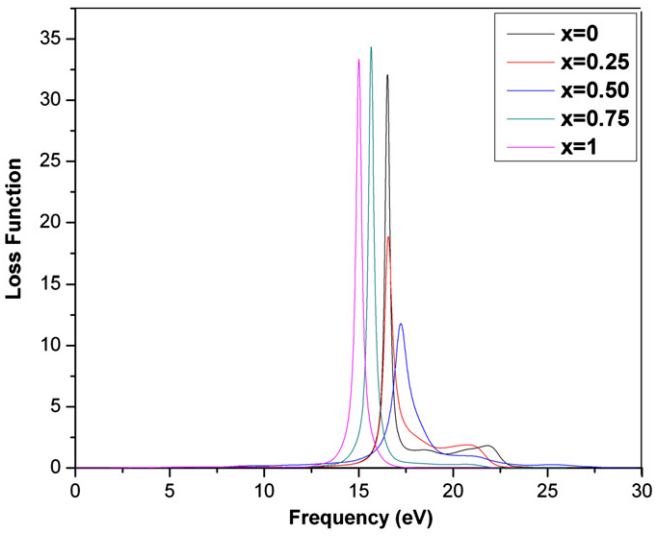

Fig. 5. Loss function of $In_xGa_{1-x}P$ alloys.

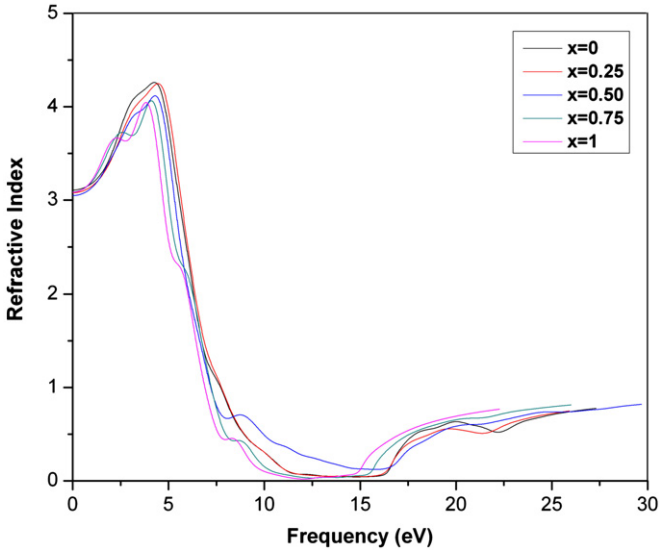

Fig. 6. Refractive Index of $In_xGa_{1-x}P$ alloys.

loss spectra do not show any distinct maxima in the range of about 0–13 eV. The reason for this is that the imaginary part of the dielectric function is still large at these energy values [25]. In the range about 13–19 eV there are some large peaks in the energy loss spectra. At such high energies the imaginary part of the dielectric function is small and the amplitude of the energy loss function becomes large.

This function has a main peak so-called Plasmon frequency for each composition x at 16.4, 16.2, 17.1, 15.6, and 15.0 eV, respectively. The composition-dependence of the Plasmon frequency does not show a regular change. However, it is seen that the highest value of Plasmon frequency is obtained for x=0.5 ($P4\bar{3}m$ structure) of $InGa_{1-x}P_x$ alloys. Fig. 6 the refractive indices $n(0)$ for $In_xGa_{1-x}P$ for each composition x are found to be 3.5, 3.4, 2.9, 3.1 and 3.0, respectively.

4. Conclusions

In summary, we have presented structural, electronic and optical properties of the $In_xGa_{1-x}P$ alloys using the first principles methods. Specifically, the lattice constants, bulk modulus and energy band gap have been calculated and consistent results are obtained. For all compositions these alloys are characterized by direct band gap materials along the Γ direction. The optical properties of the $In_xGa_{1-x}P$ alloys have been presented in detail. The investigation shows that as In composition increases in the alloys, compressibility increases whereas bulk modulus, lattice constant, band gap energy and refractive index decrease. These results are also consistent with the Vegard's law. It is hoped that the present findings may provide reliable data for producing optoelectronic devices.

Acknowledgements

The authors would like to thank Professor Mehmet KASAP and Assistant Researcher Murad Sherzad Othman for some helpful suggestions and discussions. This work is supported by the Scientific and Technical Research Council of Turkey (TUBITAK).

References

[1] P. Hohenberg, W. Kohn, Phys. Rev. B 136 (1964) 864.
[2] M. Passlack, M. Hong, J.P. Mannaerts, R.L. Opila, S.N.G. Chu, N. Moriya, F. Ren, J. Kwo, IEEE Trans. Electron Devices 44 (1997) 214.
[3] Y. Xuan, Y.Q. Wu, H.C. Lin, T. Shen, in: Proceedings of the 65th Annual Device Research Conference Digest, 2007, p. 207.
[4] J.J. Rosenberg, M. Benlamri, P.D. Kirchner, J.M. Woodall, G.D. Pettit, IEEE Electron Device Lett. 6 (1985) 491.
[5] S.F. Cheng, Y. Sun, D.C. Law, S.B. Visbeck, R.F. Hicks, Surf. Sci. 600 (2006) 2924.
[6] S. Hayashi, M. Nangu, T. Morikuni, N.S. Takahashi, J. Cryst. Growth 311 (2009) 842.
[7] I.V. Urgaftman, J.R. Meyer, J. Appl. Phys. 89 (2001) 5817.
[8] A. Ben Fredj, M. Debbichi, M. Said, Microelectronic J. 38 (2007) 860.
[9] J. Mori, E.A. Fitzgerald, J. Appl. Phys. 105 (2009) 013107.
[10] M.D. Segall, P.J.D. Lindan, M.J. Probert, C.J. Pickard, P.J. Hasnip, S.J.C. Clark, J. Phys. Condens. Matter 17 (2002) 27.
[11] W. Kohn, L.J. Sham, Phys. Rev. 140 (1965) 1133.
[12] T. Liou, Ch.Yang Lin, S.Yen, Opt. Commun. 249 (2005) 217.
[13] B.K. Agrawal, J. Phys. Condens. Matter 9 (1997) 176.
[14] M.C. Payne, M.P. Teter, D.C. Allen, T.A. Arias, J.D. Joannopolous, Rev. Mod. Phys. 64 (1992) 1045.
[15] H.J. Monkhorst, J.D. Pack, Phys. Rev. B 13 (1976) 5188.
[16] M. Oloumi, C.C. Matthai, J. Phys. Condens. Matter 2 (1990) 5153.
[17] S.Q. Wang, H.Q. Yes, Phys. Rev. B 66 (2002) 235111.
[18] K.H. Hellwege, O. Madelung, Landolt- Bornstein, Semiconductors: (Physics of Group IV Elements and III–V Compounds). New Series, Group III, 17, Pt. a Springer Verlag, Berlin, 1982 p. 602.
[19] H. Akkus, Amirullah M Mamedov, J. Phys. Condens. Matter 19 (2007) 116207.
[20] J. Sun, H.T. Wang, Phys. Rev. B 71 (2005) 125132.
[21] F. Wooten, in: Optical Properties of Solids, Academic, New York, 1972.
[22] Y. Shena, Z. Zhou, J. Appl. Phys. 103 (2008) 074113.
[23] J. Li, S.H. Wei, S.H. Li, J.B. Xia, Phys. Rev. B 74 (2006) 417.
[24] N. Serpone, D. Lawless, R. Khairutdinov, J. Phys. Chem. 99 (1995) 16646.